Molecular Genetics and Metabolism 137 (2022) 192–200

Contents lists available at ScienceDirect

Molecular Genetics and Metabolism

journal homepage: www.elsevier.com/locate/ymgme

In vitro activity of cysteamine against SARS-CoV-2 variants

Jess Thoene [a,*], Robert F. Gavin [b], Aaron Towne [c], Lauren Wattay [d], Maria Grazia Ferrari [d], Jennifer Navarrete [d], Ranajit Pal [d]

[a] Division of Pediatric Genetics, University of Michigan, United States of America
[b] Michigan Trans Tech, United States of America
[c] Mechanical Engineering, College of Engineering, University of Michigan, United States of America
[d] BIOQUAL, Rockville, MD, USA

ARTICLE INFO

Article history:
Received 1 April 2022
Received in revised form 29 August 2022
Accepted 30 August 2022
Available online 05 September 2022

Keywords:
Cysteamine
Orphan drug
SARS-CoV-2
Disulfides
Viral inhibition
Nasal spray

ABSTRACT

Global COVID-19 pandemic is caused by infection with severe acute respiratory syndrome coronavirus 2 (SARS-CoV-2). Continuous emergence of new variants and their rapid spread are jeopardizing vaccine countermeasures to a significant extent. While currently available vaccines are effective at preventing illness associated with SARS-CoV-2 infection, these have been shown to be less effective at preventing breakthrough infection and transmission from a vaccinated individual to others. Here we demonstrate broad antiviral activity of cysteamine HCl *in vitro* against major emergent infectious variants of SARS-CoV-2 in a highly permissible Vero cell line. Cysteamine HCl inhibited infection of wild type, alpha, beta, gamma, delta, lambda, and omicron variants effectively. Cysteamine is a very well-tolerated US FDA-approved drug used chronically as a topical ophthalmic solution to treat ocular cystinosis in patients who receive it hourly or QID lifelong at concentrations 6 times higher than that required to inhibit SARS CoV-2 in tissue culture. Application of cysteamine as a topical nasal treatment can potentially1) mitigate existing infection 2) prevent infection in exposed individuals, and 3) limit the contagion in vulnerable populations.

© 2022 Elsevier Inc. All rights reserved.

1. Introduction

1.1. SARS overview

Severe acute respiratory syndrome coronavirus (SARS-CoV-2) first emerged in humans during late 2019 in Wuhan, China, and transmitted globally leading to the Coronavirus Disease 19 (COVID19) pandemic. As of March 2022, COVID-19 has in resulted in 528,816,317 infections and over 6 million deaths globally [1]. Morbidity and mortality continue to grow due to the emergence of new infectious variants. SARS-CoV-2 is a highly contagious virus transmitted primarily *via* respiratory droplets. The infection typically results in a wide range of clinical outcome from an asymptomatic state to respiratory failure leading to multiorgan failure and death. While several vaccines have been developed and administered globally, the efficacy of such vaccines against the emergent variants has come into question. Moreover, hesitancy to be vaccinated has also complicated global effort successfully to control the pandemic [2].

Clearly, highly effective therapeutic and preventive strategies are needed, along with vaccines, to control the pandemic.

Here we present data showing *in vitro* inhibition of the major currently known SARS-CoV-2 variants by cysteamine.

1.2. Cysteamine overview

Cysteamine, 2-aminoethanethiol, is a simple aliphatic compound which was first used in man as an antidote to acetaminophen poisoning [3]. It was subsequently developed as a treatment for cystinosis after it was found to deplete cultured cystinosis fibroblasts of stored lysosomal cystine, which is the hallmark of cystinosis. Cystinosis is inherited as an autosomal recessive inborn error of lysosomal cystine transport, and characterized chiefly by failure to thrive, progressive renal failure and ESRD by age 10 years [4]. In 1994 USFDA NDA approval was granted for cysteamine to treat cystinosis and it also received FDA designation as one of the first Orphan Products [5]. Currently, Cysteamine is FDA and EMA approved and administered to patients in oral and topical forms to treat systemic and ophthalmic manifestations of cystinosis. Cysteamine is given orally in the systemic treatment of cystinosis. The usual oral dose in children is 50–60 mg/kg/d, and 1.3–1.6 g/m^2/d in adults. These doses yield peak blood cysteamine concentrations of ~50–70 μM 60 min after an oral dose [6,7]. The corneal crystalline keratopathy of cystinosis is treated with cysteamine eyedrops [8]. This treatment is administered 4–8 times per day and continued

* Corresponding author.
E-mail address: jthoene@umich.edu (J. Thoene).

https://doi.org/10.1016/j.ymgme.2022.08.009
1096-7192/© 2022 Elsevier Inc. All rights reserved.

life-long. Cysteamine has been administered intravenously to two cystinosis patients for 1–10 months [9,10]. It is also marketed as a 5% cream used cosmetically to treat melasma [11].

Approximately 800 patients in the United States have nephropathic cystinosis and are on chronic oral and ophthalmic cysteamine therapy, which has become the standard of care since FDA approval. As a genetic disease, cysteamine is required life-long to treat the renal and extra-renal manifestations of cystinosis which include, in addition to progressive renal failure and corneal keratopathy, distal myopathy, neurocognitive disorders, pulmonopathy, endocrinopathy, diabetes, and metabolic bone disease. The general incidence is 1/100,000 live births, although some populations have a higher incidence [12]. Prior to approval of cysteamine for treatment of cystinosis, the average native kidney survival was <10 years. Currently, with cysteamine, native renal survival can be expected to age 20 years or longer.

1.3. Cysteamine antiviral effects

1.3.1. Against HIV

Cysteamine is able to inhibit infectivity of HIV-1 *in vitro* by inhibiting the binding of gp120 with CD4 lymphocytes *via* disulfide reduction of gp`120 [13], and also acting to inhibit the virus intracellularly *in vitro* [14].

1.3.2. Against SARS

As of Jan 2022, Omicron comprised 85% of COVID 19 cases. It has displayed >30 mutations in the spike protein, of which half are in the receptor binding domain [15]. Importantly, none of the reported mutations involve cysteine residues [16] which are required to form the 14 disulfide bonds [15] in the spike protein to maintain RBD structural integrity and permit binding to the ACE2 receptor, which is required for virus entry into the cell. Grishin, et al. [17] reported *in vitro* studies of reducing agents (tris(2-carboxyethyl)phosphine (TCEP) and dithiothreitol (DTT)), which deformed the RBD secondary structure, reducing the melting temperature from 52 °C to 36–39 °C, and lowering the binding affinity by 2 log units. These agents also inhibited viral replication *in vitro* in the low mM range. Hati et al., using molecular dynamic simulation of the interaction between the spike protein and the ACE2 receptors found that the binding affinity for the interaction was significantly impaired when the disulfide bonds of both the spike protein and the ACE2 receptor were reduced to thiols [18].

The essential nature of the disulfide bonds is also supported by the evolution of the virus through various host species which does not disturb the disulfide bonds, [19]. Therefore, it is likely that altering these bonds decreases the reproductive fitness of the virus.

Recently it has been shown that cysteamine is capable of inhibiting infectivity of SARS-CoV-2 by inhibiting the binding of S1 protein to ACE-2 receptor [20]. Cysteamine and its disulfide cystamine also display anti-inflammatory effects, reducing SARS-CoV2 specific interferon-gamma production [21], In this report we define the inhibitory activity of cysteamine *in vitro* against major variants of SARS-CoV-2 that have emerged so far and find that cysteamine inhibits them at concentrations less than that currently approved by USFDA for topical ophthalmic use.

2. Methods

2.1. Cells and virus

Vero-TMPRSS2 cells used in the infection assay were provided by the Vaccine Research Center (NIH). The use of this cell line in SARS-CoV-2 infection assay is described elsewhere [22]. Cells were maintained in Dulbecco's modified Eagle's Medium (DMEM) supplemented with 10% fetal bovine serum (FBS), L-glutamine, 1% penicillin/streptomycin and puromycin (10 μg/ml). Wild type and the variants stocks of SARS-CoV-2 were expanded from the seed stocks in Calu-3 cells by infecting at varying multiplicity of infection in EMEM medium containing 2% FBS, L-glutamine and penicillin/streptomycin. Virus was isolated by harvesting the cell free culture supernatant three to four days after infection depending upon the concentration of the nucleocapsid (NP) protein present in the supernatant as measured by the antigen capture kit (My BioSource). Expanded stocks were shown to be free from the adventitious agent. Identity of each stock was confirmed by deep sequencing.

Viruses used in this study include:

Wild type SARS-CoV-2 (P4) isolate USA-WA1/2020 from BEI resources NR-52281; Alpha variant CoVID-19 (2019-nCoV/USA/CA_CDC_5574/2020) from BEI Resources NR-54011; Beta variant CoVID-19 (2019-nCoV/South Africa/KRISP-K005325/2020) from BEI Resources NR-54974; Gamma variant CoVID-19 (hCoV-19/Japan/TY7–501/2021) TY7–503 p1 (Dr. Takaji Wakita, National Institute of Infectious Diseases, Japan); Delta variants hCOV-19/USA/PHC658/2021 (B.1.617.2) from BEI Resources NR-55612 (subvariant 1); NR-55674 (subvariant 2) and NR-55694 (subvariant 3); Lambda variant hCoV-19/Peru/un-CDC-2-4,069,945/2021 (Lineage C.37) from BEI Resources NR-55656;

Omicron variants hCoV-19/USA/MD-HP20874/2021 (Lineage B.1.1.529) from BEI resources NR56462 (subvariant 1) and from Emory University (subvariant 2).

Infectivity of expanded stocks was determined by plaque forming assay in Vero-TMPRSS2 cells. Infectivity titer (pfu/ml) of each stock used in this study was 3.7×10^7 pfu/ml for wild type; 1.3×10^6 pfu/ml for alpha; 4.9×10^7 pfu/ml for beta; 1.8×10^7 pfu/ml for gamma; 2.2×10^7 pfu/ml for delta (subvariant 1), 2.9×10^7 pfu/ml for delta (subvariant 2), 2.0×10^7 pfu/ml for delta (subvariant 3); 1.8×10^7 pfu/ml for lambda; 2.9×10^7 pfu/ml for omicron (subvariant 1) and 4.8×10^6 pfu/ml for omicron (subvariant 2).

2.2. Cytotoxicity assay

To evaluate the cytotoxicity of cysteamine HCl (ACIC Pharmaceuticals Inc. Brantford, Canada), VeroTMPRSS2 cells (25,000 cells/well) were plated overnight in a 96 well plate in Dulbecco's modified Eagle's medium (DMEM) supplemented with 10% FBS, L-glutamine, 1% penicillin/streptomycin and puromycin (10 μg/ml), and the method used in virus inhibition assay was duplicated, using the same concentrations of cysteamine HCl. The cells were preincubated with Dulbecco's modified Eagle's medium (DMEM) supplemented with 2% FBS, L-glutamine, 1% penicillin/streptomycin and puromycin (10 μg/ml) (complete DMEM medium) for 2 h at 37 °C in 5% CO2 in 100 μl medium and then transferred to wells containing Vero-TMPRSS2 cells. After 1 h of incubation, medium from each well was removed and 100 μl of complete DMEM medium containing either no cysteamine HCl or 20% of the original concentration of cysteamine HCl was added to mimic the condition of the infection assay method. The plates were then cultured for 72 h at 37 °C in 5% CO2. Cytotoxicity was measured by adding 100 μl of Cell titer glow (Promega) reagent and incubated for 15 min at room temperature. Luminescence endpoint was read in a plate reader (Biotek Cytation 5). Percent cytotoxicity was calculated based on the luminescence reading of cysteamine HCl-treated wells compared to the medium only treated control wells.

2.3. Thiol quantitation

Measurement of free sulfhydryl concentration in the infection assay was performed in Vero-TMPRSS2 cells (25,000 cells/well) plated overnight in a 96 well plate in Dulbecco's Modified Eagle's Medium.

(DMEM) supplemented with 10% FBS, glutamine, 1% penicillin/streptomycin and puromycin (10 μg/ml). Thiol concentration at the same intervals as cells infected with virus was determined by Ellman's reagent (5,5′-dithio-bis-2-nitrobenzoic acid, DTNB, Sigma) by reading the optical density at 412 nm in a plate reader (Biotek Cytation 5) as described elsewhere (https://www.bmglabtech.com/ellmansassay-for-in-solution-quantification-of-sulfhydryl-groups/), and was calculated

based on a standard curve generated with the known concentrations of cysteamine HCl.

2.4. Virus inhibition assay

Antiviral activity of cysteamine HCl was assessed in a biosafety level 3 facility under compliance with BIOQUAL's health and safety procedures using inhibition of virus infection on plaque formation, VeroTMPRSS2 cells (175,000 cells per well) were added into 24 well plates in DMEM medium containing 10% FBS, L-glutamine, puromycin (10 μg/ml) and penicillin/streptomycin and the plates were cultured overnight at 37 °C in 5% CO2. For assays measuring dose dependent inhibition of infection, doses of SARS-CoV-2 (see Fig. 3) capable of forming measurable number of plaques in the control wells were preincubated with different concentrations of cysteamine HCl at 37 °C for 2 h in a total volume of 600 μl of complete DMEM medium. Cysteamine HCl/virus mixture was then transferred to each well of a 24 well plate of Vero-TMPRSS2 cells in a total volume of 250 μl and incubated for 1 h at 37 °C in 5% CO2. Each well was then overlaid with 1 ml of culture medium containing 0.5% methylcellulose and incubated for 3 days at 37 °C in 5% CO2. The plates were subsequently fixed with methanol at 20 °C for 30 min and stained with 0.2% crystal violet for 30 min at room temperature. Plaques in each well were manually scored. Inhibitory potency measured as absolute IC50 was defined as the concentration of cysteamine HCl that resulted in 50% reduction in the number of plaques compared to the untreated controls. The IC_{50} values were calculated using GraphPad Prism 9 program choosing nonlinear regression in a Dose-Response curve. For evaluating the kinetic of virus inactivation both 5 mM and 10 mM concentrations of cysteamine HCl were pre-incubated with SARS-CoV-2 for 0, 15, 30, 60 and 90 min and the mixture was then transferred to Vero-TMPRSS2 cells (175,000 cells per well) previously cultured overnight in a 24 well plate in DMEM medium containing 10% FBS, glutamine, puromycin (10 μg/ml) and penicillin/streptomycin. Remaining steps of the infection assay were as described above.

2.5. Inhibition of binding of S1 protein and the live virus to Vero-TMPRSS2 cells in the presence of cysteamine

Binding of S1 protein to Vero-TMPRSS2 cells was measured by flowcytometric assay. 2×10^6 Vero-TMPRSS2 cells were incubated with S1 protein (Sino Biologicals) from 100 to 1000 ng/ml in 500 μl FACS binding buffer (BD Biosciences) for 60 min at 37 °C, with shaking. To remove unbound S1 protein, cells were centrifuged, supernatant removed, and the pellet was washed twice with the FACS binding buffer. For staining the cell pellet was resuspended in 200 μl FACS binding buffer and stained using 5 μl (0.2 mg/ml) of anti-S1-Alexa Fluor-488 antibody (R&D Systems) following manufacturer instructions. The stained cell suspension was then transferred to a FACS tube, washed twice, and analyzed *via* a Cytek Aurora flow cytometer (Cytek). Flow data was analyzed with FlowJo software (BD).

To assay binding of S1 protein to Vero-TMPRSS2 cells in the presence of cysteamine-HCl, S1 protein (100 or 200 ng/ml) was preincubated with either no cysteamine (control) or with varying concentrations (0.31 to 10 mM) of cysteamine in 600 μl FACS binding buffer for 60 min at 37 °C with shaking. Each solution containing either medium or cysteamine-treated S1 protein (500 μl) solution was then transferred to a tube containing Vero-TMPRSS2 cells (2×10^6 cells) and the binding assay was performed as described above.

Binding of live virus to the Vero-TMPRSS2 cells was determined by flow cytometry. Varying plaque forming units (pfu) of SARS-CoV2 (Washington isolate) were preincubated with 500 μl of complete DMEM medium containing 2% FBS, L-glutamine, 1% penicillin/streptomycin and puromycin (10 μg/ml) containing either none or 5 mM cysteamine HCl for 90 min. Medium from each tube was then transferred to a separate tube containing Vero-TMPRSS2 cells (1×10^6) to achieve varying MOI of infection as shown in the Results. The cell pellets were resuspended and incubated for 60 min at 37 °C with intermittent shaking. To remove unbound virus, cells were centrifuged, supernatant removed, and the pellet washed twice with the FACS binding buffer. For staining the cell pellet was resuspended in 195 μl FACS binding buffer and stained using 5 μl (0.2 mg/ml) of anti-S1-Alexa Fluor-488 antibody (R&D Systems) following manufacturer's instruction. The stained cell suspension was then transferred to a FACS tube, washed twice, and treated with 250 μl of 1% paraformaldehyde solution for 30 min at 37 °C to inactivate live virus. Binding of anti-S1 antibody to the Vero-TMPRSS2 cells was then analyzed using a Cytek Aurora flow cytometer (Cytek) and the flow data was analyzed with FlowJo software (BD).

3. Results

3.1. In vitro toxicity of Cysteamine HCl

Cytotoxicity of cysteamine HCl in Vero-TMPRSS2 cells was determined to select the concentrations to be used in the dose response virus inhibition assay. Cysteamine HCl was preincubated in medium for 2 h followed by a one-hour incubation with Vero-TMPRSS2 cells. The mixture of cysteamine HCl and medium then was removed, and the cells cultured in fresh medium for 72 h, following which the viability of the cells was determined as described in Methods. As shown in Fig. 1A, no significant toxicity was noted below 20 mM cysteamine HCl while some toxicity was noted with 50 mM concentration. To determine if prolonged incubation of Vero-TMPRSS2 with cysteamine as done for the plaque assay would induce cytotoxicity in the target cells, cysteamine HCl was pre-incubated with medium for 2 h followed by incubation with Vero-TMPRSS2 cells for one hour. The culture medium was then diluted fivefold as done for the plaque assay and the cytotoxicity was measured after 72 h. Under these conditions, some cytotoxicity was observed at 50 mM concentrations of cysteamine HCl (Fig. 1B).

3.2. In vitro stability of Cysteamine

Because free thiols rapidly oxidize in tissue culture medium, the concentration of free thiol in the culture was measured by Elman's reagent over a period of 72 h. As shown in Fig. 2, there is progressive loss of thiol concentration during this interval. Clearly, no appreciable change in the concentration of free sulfhydryl group was detected both during the pre-incubation of cysteamine HCl with virus for two hours and during the infection step when the virus/cysteamine HCl mixture was incubated with VeroTMPRSS2 cells for an additional hour. However, a sharp drop in the concentration of -SH group was noted between 24 h and 72 h of incubation.

3.3. Inhibition of SARS-CoV-2 variants by Cysteamine

To determine dose dependent inhibition of SARS-CoV-2 by cysteamine HCl, Vero-TMPRSS2 was selected, because this cell line is known to be highly permissible to both wild type and the six variants tested in this study. Moreover, these viruses were shown to produce defined plaques when assayed in this cell line [22]. As described in the Materials and Method section, SARS-CoV-2 was pre-incubated with different concentrations of cysteamine HCl at 37 °C in 5% CO2 for 120 min and the mixture was then added to Vero-TMPRSS2 cells. After one hour of infection the plates were overlaid with 0.5% of methyl cellulose overlay and the plaques were developed and scored after 72 h. For controls, virus was treated the same way with medium lacking cysteamine HCl. Positive control, using anti-RBD rabbit polyclonal IgG was and assayed in an identical manner. Dose response curves as well as the IC50 values are shown in Fig. 3 and Table 1. Wild type WA strain as well as the alpha, beta, gamma and lambda variants were inhibited in a dose dependent manner compared to the control infection with IC50 values ranging from 1.252 mM for wild type to 1.528 mM for alpha (Fig. 3A),

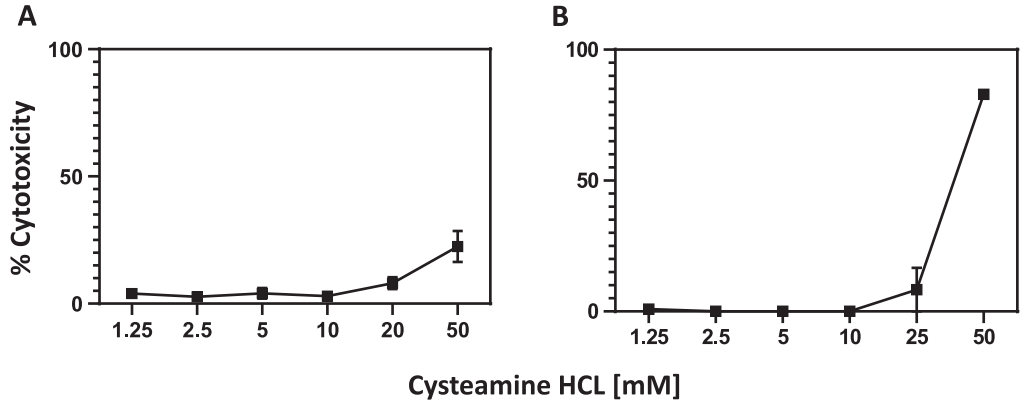

Fig. 1. Cytotoxicity of cysteamine HCl in Vero-TMPRSS2 cells. Cysteamine HCl was preincubated with Dulbecco's modified Eagle's medium (DMEM) supplemented with 2% FBS, Lglutamine, 1% penicillin/streptomycin and puromycin (10 μg/ml) for 2 h at 37 °C in 5% CO2 in 100 μl medium and then transferred to the wells containing Vero-TMPRSS2 cells. After 1 h of incubation medium from each well was removed and 100 μl of complete DMEM medium containing either no cysteamine-HCl (A) or 20% of the original concentration of cysteamine-HCl was added to mimic the condition of the infection assay method (B). Cells were cultured for 72 h at 37 °C in 5% CO2 and cytotoxicity measured as described in the Method section.

0.799 mM for beta, 0.8602 mM for lambda and 1.976 mM for gamma variant (Fig. 3B). A similar pattern of inhibition of infection was noted when three different subvariants of delta variant was treated with different concentrations of cysteamine HCl (Fig. 3C) with IC50 value of 1.066 mM for subvariant 1, 1.7 mM for subvariant 2 and 1.373 mM for subvariant 3. Similarly, two subvariants of omicron were also inhibited by cysteamine-HCl with IC 50 value of 0.671 mM for subvariant 1 and 1.006 mM for subvariant 2 (Fig. 3D). Positive controls using anti-rabbit RBD polyclonal IgG inhibited infection of all viruses in a dose dependent manner (data not shown).

To determine the duration of incubation of virus with cysteamine HCl required for maximal inhibition, the Delta variant was pre-incubated with either 5- or 10 mM concentration of cysteamine HCl for 0, 15, 30, 60 and 90 min. The mixture was then added to Vero-TMPRSS2 cells and infection continued for an additional 60 min resulting in a total association time of virus with cysteamine HCl of 60, 75, 90, 120 and 150 min. As shown in Fig. 4, inhibition of delta variant was produced by both 5 and 10 mM cysteamine HCl under these conditions, with maximum inhibition at 10 mM when the virus and cysteamine HCl was incubated for 150 min. The level of inhibition of infection in this assay was slightly less than that observed in the dose response inhibition assay (Fig. 3C) because the association time of virus with cysteamine HCl in this assay was 150 min when assayed compared to 180 min in Fig. 3C.

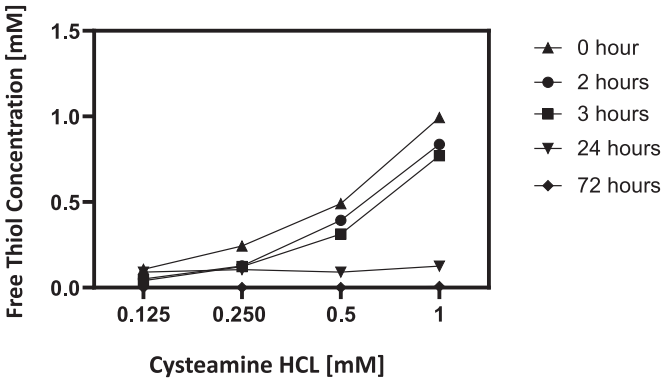

Fig. 2. Cysteamine Stability in Tissue Culture: The free thiol content of four concentrations of cysteamine HCl were measured at the initiation of pre-incubation with virus (0 h), after pre-incubation with virus (2 h), during incubation of cysteamine HCl/virus mixture with Vero-TMPRSS2 cells 3, 24 and 72 h post infection as described in the Method Section.

3.4. Inhibition of binding of live virus and S1 protein to Vero-TMPRSS2 cells by Cysteamine

Inhibition of SARS-CoV2 infection by cysteamine led us to evaluate the binding of S1 protein to the Vero-TMPRSS2 cells in the presence of cysteamine using the conditions used in the infection assay. Initially we determined the optimal concentration of S1 protein required to bind to the Vero-TMPRSS2 cells at a non-saturating level. To this end, varying concentrations of S1 protein were incubated with Vero-TMPRSS2 cells for 60 min at 37 °C and the bound S1 protein was detected using Alexa Four-488 conjugated anti-S1 antibody as described in the Method section. As shown in Fig. 5A, the binding of S1 protein to Vero-TMPRSS2 cells increased with increasing concentration of S1 protein with saturating level of binding noted above 500 ng/ml concentration. Based on this binding profile we selected 100 ng/ml and 250 ng/ml for evaluating the effect of cysteamine on binding of S1 to the target cells. For determining the cysteamine effect on binding, we preincubated S1 protein with varying concentrations of cysteamine as used in the infection assay for 60 min at 37 °C following which the mixture was incubated with Vero-TMPRSS2 cells for an additional 60 min at 37 °C to mimic viral infection. The level of bound S1 protein was then assayed by flow cytometry after staining with Alexa Four-488 conjugated anti-S1 antibody. The scatter plots used for such binding are shown in Fig. 5B and the corresponding dose-dependent inhibition curve is shown in Fig. 5C. It is clear from both figures that the treatment of S1 protein with cysteamine inhibited the binding of S1 protein to the Vero-TMPRSS2 cells in a concentration dependent manner with profound inhibition noted at 5 and 10 mM cysteamine, especially incubation with 100 ng/ml S1 protein concentration (Fig. 5C). In this experiment the gating strategy for all the scatter plots was chosen using unstained controls cells not treated with cysteamine. To ensure that the inhibition of binding of S1 protein was not attributable to a shift of the cell population following cysteamine treatment, experiments were conducted to measure the binding of S1 protein (250 ng/ml) in the presence of both 5- and 10 mM cysteamine using the above condition except for the gating strategy. In this experiment gating strategy was established using unstained cysteamine-treated cells for the cysteamine group and the medium treated cells for the controls. As shown in the scatter plot (Fig. 5D), similar inhibition of binding of S1 protein to Vero-TMPRSS2 cells was noted in the presence of both 5 and 10 mM cysteamine after gating using cysteamine-treated unstained cells compared to the control cells in medium. This clearly demonstrates that the inhibition of S1 binding to the Vero-TMPRSS2 cells by cysteamine was not attributed to the altered gating attributed to the

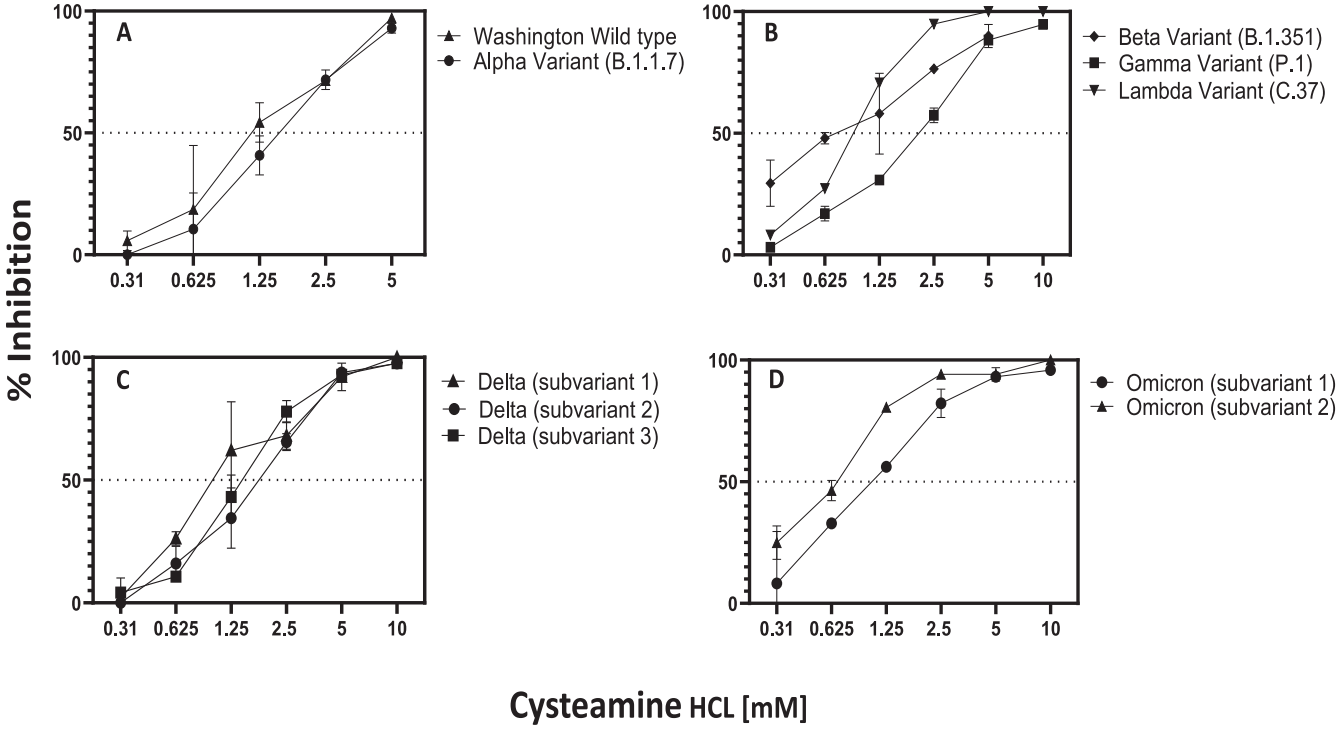

Fig. 3. Dose dependent inhibition of infection of wild type and SARS-CoV-2 variants by cysteamine HCl: (A) Wild type (25 pfu/well), alpha (125 pfu/well); (B) beta (18.75 pfu/well), gamma (25 pfu/well); lambda (60 pfu/well); (C) delta subvariant 1 (37.5 pfu/well), subvariant 2 (48pfu/ml), subvariant 3 (42 pfu/ml); (D) omicron B1.1, subvariant 1 (16.8pfu/well) and subvariant 2 (24pfu/well). Virus was preincubated with varying concentrations of cysteamine HCl at 37 °C for 2 h in a total volume of 600 μl of complete DMEM medium as shown in the figure. Cysteamine HCl/virus mixture was then transferred to each well of Vero-TMPRSS2 cells in a total volume of 250 μl and incubated for 1 h at 37 °C in 5% CO2. Each well was then overlaid with 1 ml of culture medium containing 0.5% methylcellulose and incubated for 3 days at 37 °C in 5% CO2 and plaques were developed and scored as described in the Method section. Mean percent inhibition +/− standard error of infection compared to the untreated control is plotted.

morphological changes of the Vero-TMPRSS2 cells by cysteamine but represents a specific inhibitory effect of cysteamine on S1 binding to the target cells.

Once the inhibition of binding of S1 protein to the Vero-TMPRSS2 was noted, we evaluated binding of live virus to the Vero-TMPRSS2 in the presence of 5 mM cysteamine-HCl. This binding was determined by measuring the binding of S1 protein from the virus to the cells by anti-S1 antibody. For this varying infectious units of SARS-CoV2 were pre-incubated with medium alone or with 5 mM cysteamine-HCl for 90 min at 37 °C in 5% CO2 and the mixture was incubated with Vero-TMPRSS2 cells for an additional 60 min at 37 °C to initiate viral infection. The level of bound S1 protein was then assayed by flow cytometry after staining with Alexa Four-488 conjugated anti-S1 antibody. The scatter plots obtained for the binding of S1 protein of virus following infection with varying MOI of infection both in the absence or in the presence of cysteamine HCl are shown in Fig. 6A and the corresponding dose response curve is presented in Fig. 6B. Clearly the number of S1-positive cells increased from 15.5% following infection with MOI 0.9 to 39% with MOI 8 due to the increased binding of S1 protein from the virus with increased MOI. Preincubation of different infectious doses of virus with 5 mM cysteamine produced a significant reduction in the

Table 1
IC_{50} values of Cysteamine HCL against wild type and major variants of SARS-CoV2. Inhibitory potency measured as IC_{50} was defined as the concentration of cysteamine-HCl that resulted in 50% reduction in the number of plaques compared to the untreated controls.

Virus	IC_{50} [mM]
Wild type (Washington)	1.252
Alpha variant	1.528
Beta variant	0.799
Gamma variant	1.976
Lambda variant	0.860
Delta variant (subvariant 1)	1.066
Delta variant (subvariant 2)	1.700
Delta variant (subvariant 3)	1.373
Omicron variant (subvariant 1)	0.671
Omicron variant (subvariant 2)	1.006

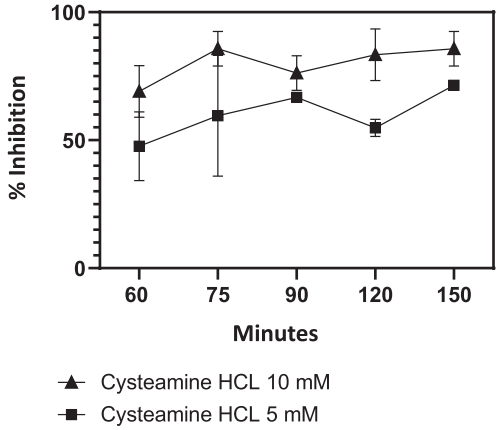

Fig. 4. Kinetics of Inhibition of delta variant infection by cysteamine HCl.
Delta variant (Subvariant 1) (37.5 pfu/ml) was preincubated with cysteamine HCl (5 or 10 mM) for 0, 15, 30, 60 and 90 min in a total volume of 600 μl of complete DMEM medium. The cysteamine HCl/virus mixture was then transferred to wells of Vero-TMPRSS2 cells in a total volume of 250 μl and incubated for 1 h at 37 °C in 5% CO2. Wells were then overlaid with 1 ml of culture medium containing 0.5% methylcellulose and plaques were developed as described in the Method section. In both assays plaques were developed and scored as described in the Method section. Mean percent inhibition of infection +/− standard error compared to the untreated control along with the total time of association of virus and cysteamine before addition of 0.5% methyl cellulose overlay was plotted.

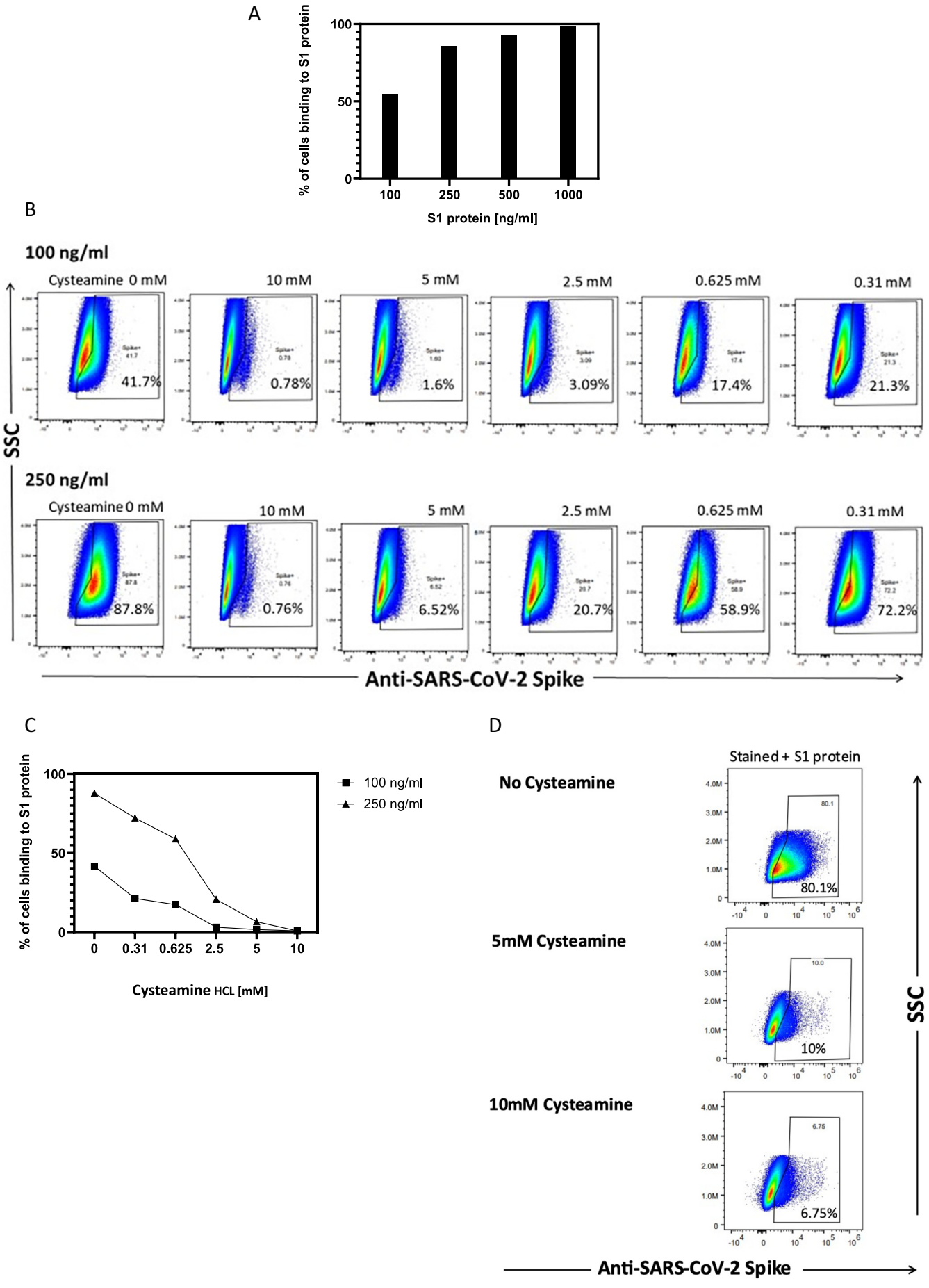
A
% of cells binding to S1 protein
100
50
0
100
250
500
1000
S1 protein [ng/ml]
B
100 ng/ml
Cysteamine 0 mM
10 mM
5 mM
2.5 mM
0.625 mM
0.31 mM
41.7%
0.78%
1.6%
3.09%
17.4%
21.3%
SSC
250 ng/ml
Cysteamine 0 mM
10 mM
5 mM
2.5 mM
0.625 mM
0.31 mM
87.8%
0.76%
6.52%
20.7%
58.9%
72.2%
Anti-SARS-CoV-2 Spike
C
% of cells binding to S1 protein
100
50
0
0
0.31
0.625
2.5
5
10
100 ng/ml
250 ng/ml
Cysteamine HCL [mM]
D
Stained + S1 protein
No Cysteamine
80.1%
5mM Cysteamine
10%
10mM Cysteamine
6.75%
SSC
Anti-SARS-CoV-2 Spike

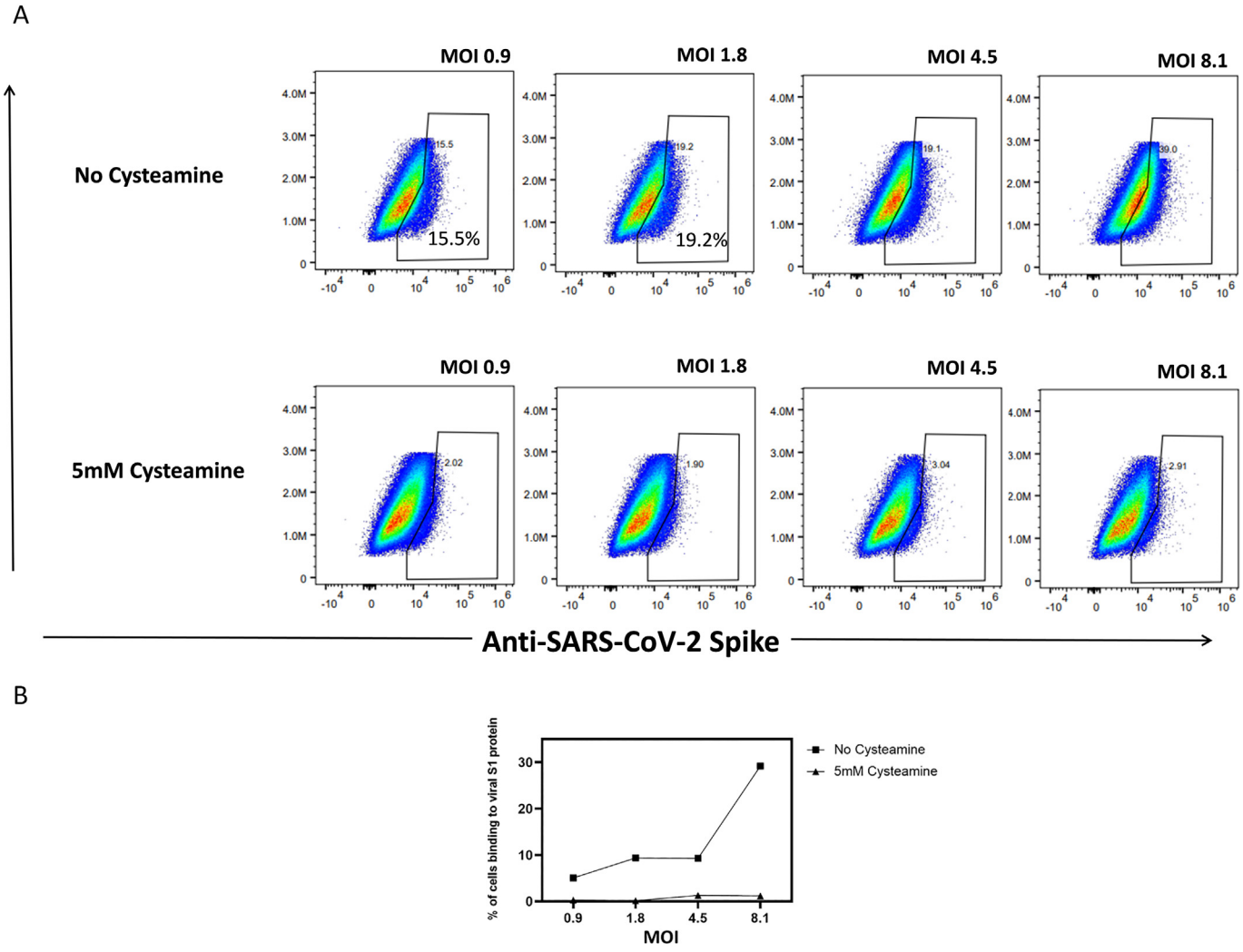

Fig. 6. Binding of virus to the Vero-TMPRSS2 in the presence of cysteamine-HCl.
(A) Scatter plots obtained for the binding of S1 protein following infection with varying MOI of infection both in the absence or in the presence of 5 mM cysteamine HCl. Varying infectious units of SARS-CoV2 (Wild type SARS-CoV-2 (P4) isolate USA-WA1/2020) were pre-incubated with medium alone or with 5 mM cysteamine-HCl for 90 min at 37 °C in 5% CO2 and the mixture was incubated with Vero-TMPRSS2 cells for an additional 60 min at 37 °C to initiate viral infection. The level of bound S1 protein was then assayed by flow cytometry after staining with Alexa Four-488 conjugated anti-S1 antibody. Percent binding represents the % of anti-S1+ cells after gating on singlets and live cells.
(B) Dose dependent inhibition of the virus binding to Vero-TMPRSS2 cells in the presence of cysteamine.
Values were normalized with the background fluorescence obtained from stained uninfected cells under appropriate conditions.

binding of S1 protein from the virus to the target cell. The inhibitory effect of cysteamine HCl on the virus binding was most pronounced when the infection was performed with 8 MOI of infection where the level of binding decreased from 39% to close to 3%. These results are consistent with the inhibition of infection by cysteamine is due to the interference of binding of virus to the target cells. This observation is in line with that made earlier by Khanna et al. [20] who showed in a solid phase ELISA, inhibition of binding of ACE-2 protein to the RBD domain of S1 protein pre-treated with cysteamine.

4. Discussion

In this study the antiviral activity of cysteamine HCl was assessed against wild type and major variants of SARS-CoV-2 that have emerged so far including the delta and omicron variants, which have spread widely throughout the world with devastating consequences [1]. These assays were conducted using Vero-E6 cells which over-express the transmembrane serine protease II (Vero-TMPRSS2), because they are highly susceptible to infection with wild type and all variants of

Fig. 5. Binding of S1 protein to Vero-TMPRSS2 cells in the presence of cysteamine. (A) Binding of varying concentrations of S1 protein to the Vero-TMPRSS2 cells. The cells were incubated for 60 min at 37 °C with concentrations of S1 protein (Sino Biologicals) from 100 to 1000 ng/ml, followed by anti-S1-Alexa Fluor-488 antibody staining as described in Methods. Percent binding is the % of anti-S1+ cells after gating on singlets and live cells. The concentrations of 250 and 100 ng/ml were selected to perform the subsequent experiments based on the non-saturating level of S1 binding (54.5–85.7%). All titration experiments were replicated twice with similar outcome. (B) Scatter plots and (C) corresponding column graphs showing the effect of cysteamine on the binding of S1 protein to the Vero-TMPRSS2 cells. S1 protein (100 or 250 ng/ml) was preincubated with varying concentrations (0.31 to 10 mM) of cysteamine for 60 min at 37 °C. For control S 1 protein was incubated with FACS binding buffer without cysteamine. Cysteamine-treated or medium treated S1 protein solution was then transferred to a tube containing Vero-TMPRSS2 cells and the binding assay was performed as described in the Methods using anti-S1-Alexa Fluor-488 antibody staining. Percent binding represents the % of anti-S1+ cells after gating on singlets and live cells. All experiments were repeated twice with comparable outcome. (D) Scatter plots evaluated the effect of cysteamine on binding of S1 (250 ng/ml) using above condition. The gating strategy selected for the analysis was done using specific unstained cells treated with medium (control) or with 5 and 10 mM cysteamine-HCL for 60 min for the respective group.

SARS-CoV2. Our results demonstrate *in vitro* antiviral activity of cysteamine against both wild type and multiple variants of SARS-CoV-2 (Fig. 3). A similar inhibition of the infectivity of SARS-CoV-2 with cysteamine was previously demonstrated [20], but with IC_{50} values lower than what was noted in our study (Table 1) We also demonstrate inhibition of binding of the spike protein and live virus to Vero-TMPRSS cells following incubation of both S1 protein and virus with cysteamine-HCl (Figs. 5 and 6).

As noted above, the spike protein of SARS-CoV-2 is reported to have fourteen disulfide bonds [19]. It is likely that cysteamine reduces the disulfide bonds leading to altered conformation and instability of the receptor binding domain. This, in turn, inhibits binding of RBD with ACE-2 receptor on the target cells [19,20]. Our results here have demonstrated such inhibition of binding of both S1 protein, and the live virus (assessed by measuring the binding of S1) to the target cells in the presence of inhibitory concentration of cysteamine HCl. Binding assays performed with the live virus used conditions like the infection assay where virus was pre-incubated with cysteamine HCl for 90 min prior to infection of Vero-TMPRSS2 cells for an additional 60 min. One difference of this binding assay performed with the live virus with that of the infection assay is that the former was performed in the suspension culture whereas the infection assay was conducted in monolayer culture. It is unlikely that this difference would influence the observation in significant way since expressions of both ACE2 and TMPRSS2 proteins were easily detectable in the suspension culture by FACS (data not shown). Clearly one of the mechanisms by which cysteamine HCl inhibits infection of SARS-CoV2 was by inhibiting the binding of virus to the target cells. However, this does not rule out additional mechanism(s) of action of cysteamine HCl as an antiviral agent. Since the disulfide residues in the RBD are uniformly conserved among the emergent variants, it is not surprising that all six variants are sensitive to inhibition by cysteamine HCl. Any viable future mutations are predicted to remain susceptible to cysteamine, as any mutations affecting the disulfide bonds would lead to reduced reproductive fitness of the virus.

Cysteamine is a free thiol with the odor and taste of rotten eggs, accounting for the olfactory and taste aversion to this medication. Despite this, cysteamine has been shown to be well tolerated when administered orally to patients with cystinosis [3]. Side effects due to oral forms are primarily limited to nausea, vomiting and gastric hyperacidity. This limits compliance in some younger patients on chronic cysteamine therapy, however 94% of patients >11 years of age reported always being compliant, compared to 50% < 11 years of age who were less [22]. Cysteamine eye drops are well tolerated and are marketed in both immediate and long-acting forms. The first ocular form to be FDA approved, Cystaran, is recommended to be given hourly while awake. A more recent, long-acting form, Cystadrops, is administered four times a day while awake. Both are well tolerated but may provoke transient burning and mild eye irritation is some patients. Both are used in lifelong treatment to maintain the corneas free of cystine crystals.

It is accepted that nasal epithelium cells located in the nasopharynx are: (i) the initial source of individual infection with SARSCoV2; (ii) the location of rapid replication and mutation of the virus, and (iii) the primary source from which the virus spreads to others. The nasal epithelium is a target for SARSCoV2 to enter and replicate *via* the concentrated ACE2 receptors on goblet cells [23]. As the virus proliferates in the nasal epithelium, lysis of epithelial cells releases virions in a logarithmic progression which then transit to the trachea, bronchi and ultimately alveoli, leading to pneumonia, devastating illness [24], and markedly greater infectivity, as measured by R_{RI} [25]. Since cysteamine is currently marketed as two well tolerated ophthalmic preparations, Cystaran ® (0.44%, = 56 mM), and Cystadrops® (0.37%, = 33 mM) the drug could feasibly be administered topically to the nasal epithelium in the concentrations used for frequent ocular administration, and which are shown to inactivate the virus *in vitro* in tissue culture in highly permissive cells at concentrations between one tenth and one sixth that currently approved for chronic ophthalmic use by US FDA (see Figs. 3 and 4). There it could act as a chemical impediment to nasal entry and thus to virus replication. Cysteamine employed as a nasal spray, cream or drops could function as both a preventative and mitigator of COVID-19 infection. The Delta variant is believed to result in significantly higher viral loads in the nasopharynx than the original virus, thus providing significantly greater opportunities for viral spread and mutation.

Reducing or eliminating the virus's ability to infect nasal epithelium cells by treatment with topical cysteamine would not only reduce its ability to sicken infected individuals, but also reduce or eliminate its ability to replicate, mutate and infect others. Nasal sprays to combat SARS Cov-2 have been proposed, including nasal administration of nitric oxide (NO) [26], carrageenan, Ivermectin, chloroquine, Niclosamide, steroids, ethyl lauroyl arginate, hypochlorous acid, povidone-iodine, antibodies, lipopeptide, and a PEGylated TLR2/6 agonist. All are in various levels of pre-clinical or clinical trials [27].

Utilization of a nasal spray as a means of administering an antiviral agent to prevent or mitigate SARSCoV-2 infection requires exposure to the antiviral for a period sufficient to inactivate the virus. Given the known dimensions of the virus (100 nm diameter), and its mass (10^{-18} kg) [28], one may apply Stokes law [29] to calculate the terminal velocity in water @ 25 °C of 5.6×10^{-9} m/s. This assumes, of course, that the virus is a perfect sphere, which it is not. The spike proteins will increase the resistance; therefore, this is an over-estimate of terminal velocity. The nasal surface area is reported at 150 cm^2 [30]. A nasal spray of 0.5 ml in each nostril, a volume well tolerated by children [31], would deliver 1 ml total volume to the nasal surface, yielding a uniform thickness of the antiviral solution of 1 cm3 / 150 cm2 = 0.0067 cm, or 67 μ (670 virion diameters). This would be traversed by a virion at terminal velocity in 11,964 s, or ~3.3 h, greater than the time required to almost completely inactivate the virus by 10 mM cysteamine in tissue culture (see Fig. 3). This assumes both uniform distribution of the nasal spray throughout the nasal epithelium, and uniform distribution of ACE2 receptors. Employing nasal spray is a potential advantage in smaller children who are averse to masks, or whose parents are opposed to vaccines.

The dwell time of virus in the film may be increased by increasing the viscosity of the excipient, which will linearly increase the dwell time [29].

5. Summary

The results presented in this communication demonstrate significant inhibition of infection by cysteamine HCl of variants of SARS-CoV-2 including delta, lambda and omicron in the highly permissible cell line Vero-TMPRSS2. Cysteamine is a well-studied drug with very good safety profile with chronic use in patients with cystinosis, and the approved concentration for topical use in ophthalmic preparations is 4 to 6 times that required for virus inhibition *in vitro*. Administration of cysteamine as a topical agent to the nasal mucosa of both pre-exposed and infected individuals may be beneficial in number of ways *via* formation of a chemical barrier. It would thus prevent virus binding and inhibit infection of ACE-2 expressing epithelial cells, thereby reducing the amount of infectious virus entering the trachea-bronchial tree, possibly mitigating the severity of the illness, and by reducing the amount of infectious virus produced in the nasal epithelium, reducing the spread of virus.

Acknowledgement

Cysteamine-HCL used in this study was provided by ACIC Pharmaceuticals Inc. (Ontario, Canada). We would like to thank Takaji Wakita from the National Institute of Infectious Diseases, Japan, for kindly providing the gamma variant and Mehul Suthar from the Emory University, USA for one of the subvariants of omicron used in this study. The rest of the virus stocks used here were obtained from BEI Resources, NIAID,

NIH as mentioned in the Materials and Methods. We would like to thank.

Shelby O'Connor, John Baczenas and Corina Valencia from the University of Wisconsin-Madison, USA for deep sequencing our in-house expanded virus stocks and Adrian Creanga from the Vaccine Research Center-NIAID, USA, for the Vero TMPRSS2 cell line.

Jess Thoene and Robert Gavin are inventors on a patent application related to the use of cysteamine for the prevention and treatment of COVID-19 infections. It is assigned to the University of Michigan, licensed by ACIC Pharmaceuticals, Inc. who funded this study. Jess Thoene is a consultant to ACIC.

References

[1] WHO, COVID-19 Dashboard, https://covid19.who.int/.
[2] G. Lobinska, A. Pauzner, A. Traulsen, et al., Evolution of resistance to COVID-19 vaccination with dynamic social distancing, Nat. Hum. Behav. 6 (2022) 193–206, https://doi.org/10.1038/s41562-021-01281-8.
[3] L.F. Prescott, R.W. Newton, C.P. Swainson, N. Wright, A.R. Forrest, H. Matthew, Successful treatment of severe paracetamol overdosage with cysteamine, Lancet 1 (1974) 588–592.
[4] J.G. Thoene, R.G. Oshima, J.C. Crawhall, D.L. Olson, J.A. Schneider, Cystinosis. Intracellular cystine depletion by aminothiols in vitro and in vivo, J. Clin. Invest. 58 (1976) 180–189.
[5] W.A. Gahl, G.F. Reed, J.G. Thoene, J.D. Schulman, W.B. Rizzo, A.J. Jonas, D.W. Denman, J.J. Schlesselman, B.J. Corden, J.A. Schneider, Cysteamine therapy for children with nephropathic cystinosis, N. Engl. J. Med. 316 (1987) 971–977.
[6] L.A. Smolin, K.F. Clark, J.G. Thoene, W.A. Gahl, J.A. Schneider, A comparison of the effectiveness of cysteamine and phosphocysteamine in elevating plasma cysteamine concentration and decreasing leukocyte free cystine in nephropathic cystinosis, Pediatr. Res. 23 (1988) 616–620.
[7] L. Tenneze, V. Daurat, A. Tibi, P. Chaumet-Riffaud, C. Funck-Brentano, A study of the relative bioavailability of cysteamine hydrochloride, cysteamine bitartrate and phosphocysteamine in healthy adult male volunteers, Br. J. Clin. Pharmacol. 47 (1999) 49–52.
[8] W.A. Gahl, J.G. Thoene, J.A. Schneider, Cystinosis, N. Engl. J. Med. 347 (2002) 111–121.
[9] W.A. Gahl, J. Ingelfinger, P. Mohan, I. Bernardini, P.E. Hyman, A. Tangerman, Intravenous cysteamine therapy for nephropathic cystinosis, Pediatr. Res. 38 (1995) 579–584.
[10] M.R. Bendel-Stenzel, J. Steinke, R. Dohil, Y. Kim, Intravenous delivery of cysteamine for the treatment of cystinosis: association with hepatotoxicity, Pediatr. Nephrol. 23 (2008) 311–315.
[11] P. Mansouri, S. Farshi, Z. Hashemi, B. Kasraee, Evaluation of the efficacy of cysteamine 5% cream in the treatment of epidermal melasma: a randomized double-blind placebo-controlled trial, Br. J. Dermatol. 173 (2015) 209–217.
[12] S. Cherqui, P.J. Courtoy, The renal Fanconi syndrome in cystinosis: pathogenic insights and therapeutic perspectives, Nat Rev Nephrol 13 (2017) 115–131.
[13] R. Barbouche, R. Miquelis, I.M. Jones, E. Fenouillet, Protein-disulfide isomerase-mediated reduction of two disulfide bonds of HIV envelope glycoprotein 120 occurs post-CXCR4 binding and is required for fusion, J. Biol. Chem. 278 (2003) 3131–3136.
[14] A. Bergamini, L. Ventura, G. Mancino, M. Capozzi, R. Placido, A. Salanitro, L. Cappannoli, E. Faggioli, A. Stoler, G. Rocchi, In vitro inhibition of the replication of human immunodeficiency virus type 1 by beta-mercaptoethylamine (cysteamine), J. Infect. Dis. 174 (1996) 214–218.
[15] L. Qu, Z. Yi, Y. Shen, L. Lin, F. Chen, Y. Xu, Z. Wu, H. Tang, X. Zhang, F. Tian, C. Wang, X. Xiao, X. Dong, L. Guo, S. Lu, C. Yang, C. Tang, Y. Yang, W. Yu, J. Wang, Y. Zhou, Q. Huang, A. Yisimayi, S. Liu, W. Huang, Y. Cao, Y. Wang, Z. Zhou, X. Peng, J. Wang, X.S. Xie, W. Wei, Circular RNA vaccines against SARS-CoV-2 and emerging variants, Cell 185 (10) (2022 May 12) 1728–1744, e16 https://doi.org/10.1016/j.cell.2022.03.044 Epub 2022 Apr 1. PMID: 35460644; PMCID: PMC8971115.
[16] Jiahui Chen, Guo-Wei Wei, Omicron BA.2 (B.1.1.529.2): High Potential to Becoming the Next Dominating Variant, https://arxiv.org/abs/2202.05031.
[17] A.M. Grishin, N.V. Dolgova, S. Landreth, O. Fisette, I.J. Pickering, G.N. George, D. Falzarano, M. Cygler, Disulfide bonds play a critical role in the structure and function of the receptor-binding domain of the SARS-CoV-2 Spike Antigen, J Mol Biol 434 (2) (2022 Jan 30) 167357, https://doi.org/10.1016/j.jmb.2021.167357 Epub 2021 Nov 12. PMID: 34780781; PMCID: PMC8588607.
[18] S. Hati, S. Bhattacharyya, Impact of thiol-disulfide balance on the binding of COVID-19 spike protein with angiotensin-converting enzyme 2 receptor, ACS Omega. 5 (26) (2020 Jun 23) 16292–16298, https://doi.org/10.1021/acsomega.0c02125 PMID: 32656452; PMCID: PMC7346263.).
[19] J. Shang, G. Ye, K. Shi, et al., Structural basis of receptor recognition by SARS-CoV-2, Nature 581 (2020) 221–224, https://doi.org/10.1038/s41586-020-2179-y.
[20] K. Khanna, W. Raymond, J. Jin, A.R. Charbit, I. Gitlin, M. Tang, A.D. Werts, E.G. Barrett, M. Cox, S.M. Birch, R. Martinelli, H.S. Sperber, S. Franz, S. Pillai, A.M. Healy, T. Duff, S. Oscarson, M. Hoffmann, S. Pohlmann, G. Simmons, J.V. Fahy, Thiol drugs decrease SARS CoV-2 lung injury in vivo and disrupt SARS-CoV-2 spike complex binding to ACE2 in vitro, bioRxiv (2021) https://doi.org/10.1101/2020.12.08.415505.
[21] T. Alonzi, A. Aiello, L. Petrone, S. Najafi Fard, M. D'Eletto, L. Falasca, R. Nardacci, F. Rossin, G. Delogu, C. Castilletti, M.R. Capobianchi, G. Ippolito, M. Piacentini, D. Goletti, Cysteamine with in vitro antiviral activity and immunomodulatory effects has the potential to be a repurposing drug candidate for COVID-19 therapy, Cells 2022 11 (2021) 52, https://doi.org/10.3390/cells11010052.
[22] G. Ariceta, E. Lara, J.A. Camacho, F. Oppenheimer, J. Vara, F. Santos, M.A. Munoz, C. Cantarell, M. Gil Calvo, R. Romero, B. Valenciano, V. Garcia-Nieto, M.J. Sanahuja, J. Crespo, M.L. Justa, A. Urisarri, R. Bedoya, A. Bueno, A. Daza, J. Bravo, F. Llamas, L.A. Jimenez Del Cerro, Cysteamine (Cystagon(R)) adherence in patients with cystinosis in Spain: successful in children and a challenge in adolescents and adults, Nephrol. Dial. Transplant. 30 (2015) 475–480.
[23] W. Sungnak, N. Huang, C. Becavin, M. Berg, R. Queen, M. Litvinukova, C. Talavera-Lopez, H. Maatz, D. Reichart, F. Sampaziotis, K.B. Worlock, M. Yoshida, J.L. Barnes, H.C.A.L.B. Network, SARS-CoV-2 entry factors are highly expressed in nasal epithelial cells together with innate immune genes, Nat. Med. 26 (2020) 681–687.
[24] Y.J. Hou, K. Okuda, C.E. Edwards, D.R. Martinez, T. Asakura, K.H. Dinnon 3rd, T. Kato, R.E. Lee, B.L. Yount, T.M. Mascenik, G. Chen, K.N. Olivier, A. Ghio, L.V. Tse, S.R. Leist, L.E. Gralinski, A. Schäfer, H. Dang, R. Gilmore, S. Nakano, L. Sun, M.L. Fulcher, A. Livraghi-Butrico, N.I. Nicely, M. Cameron, C. Cameron, D.J. Kelvin, A. de Silva, D.M. Margolis, A. Markmann, L. Bartelt, R. Zumwalt, F.J. Martinez, S.P. Salvatore, A. Borczuk, P.R. Tata, V. Sontake, A. Kimple, I. Jaspers, W.K. O'Neal, S.H. Randell, R.C. Boucher, R.S. Baric, SARS-CoV-2 reverse genetics reveals a variable infection gradient in the respiratory tract, Cell 182 (2) (2020 Jul 23) 429–446 , e14 https://doi.org/10.1016/j.cell.2020.05.042 Epub 2020 May 27. PMID: 32526206; PMCID: PMC7250779.
[25] K. Ito, C. Piantham, H. Nishiura, Predicted dominance of variant Delta of SARS-CoV-2 before Tokyo Olympic games, Japan, July 2021, Euro Surveill. 26 (27) (2021 Jul) 2100570, https://doi.org/10.2807/1560-7917.ES.2021.26.27.2100570 PMID: 34240695; PMCID: PMC8268651.
[26] S. Winchester, S. John, K. Jabbar, I. John, Clinical efficacy of nitric oxide nasal spray (NONS) for the treatment of mild COVID-19 infection, J. Inf. Secur. 83 (2021) 237–279.
[27] B. Pilicheva, R. Boyuklieva, Can the nasal cavity help tackle COVID-19? Pharmaceutics. 13 (10) (2021 Oct 3) 1612, https://doi.org/10.3390/pharmaceutics13101612 PMID: 34683904; PMCID: PMC8537957.
[28] Y.M. Bar-On, A. Flamholz, R. Phillips, R. Milo, SARS-CoV-2 (COVID-19) by the numbers, Elife. 9 (2020), e57309 , Published 2020 Apr 2 https://doi.org/10.7554/eLife.57309.
[29] G.K. Batchelor, An Introduction to Fluid Dynamics, Cambridge University Press, 1967 ISBN 0–521–66396-2.
[30] L. Illum, Transport of drugs from the nasal cavity to the central nervous system, Eur. J. Pharm. Sci. 11 (2000) 1–18.
[31] D.S. Tsze, M. Ieni, D.B. Fenster, J. Babineau, J. Kriger, B. Levin, P.S. Dayan, Optimal volume of administration of intranasal midazolam in children: a randomized clinical trial, Ann. Emerg. Med. 69 (2017) 600–609.